



ELSEVIER

Contents lists available at ScienceDirect

Applied Surface Science

journal homepage: [www.elsevier.com/locate/apsusc](http://www.elsevier.com/locate/apsusc)

# Flexible conducting platforms based on PEDOT and graphite nanosheets for electrochemical biosensing applications

Juliana Scotto<sup>a,b</sup>, Esteban Piccinini<sup>a</sup>, Catalina von Bilderling<sup>a</sup>, Lucy L. Coria-Oriundo<sup>c</sup>, Fernando Battaglini<sup>c</sup>, Wolfgang Knoll<sup>d,e</sup>, Waldemar A. Marmisolle<sup>a,\*</sup>, Omar Azzaroni<sup>a,f,\*</sup>

<sup>a</sup> Instituto de Investigaciones Fisicoquímicas Teóricas y Aplicadas, Departamento de Química, Facultad de Ciencias Exactas, Universidad Nacional de La Plata, CONICET, CC 16 Suc. 4, La Plata B1904DPI, Argentina

<sup>b</sup> Instituto de Ciencias de la Salud, Universidad Nacional Arturo Jauretche, Av. Calchaquí 6200, Florencio Varela, Buenos Aires, Argentina

<sup>c</sup> INQUIMAE, Departamento de Química Inorgánica, Analítica y Química Física, Facultad de Ciencias Exactas y Naturales, Universidad de Buenos Aires, Ciudad Universitaria, Buenos Aires, Argentina

<sup>d</sup> CEST – Competence Center for Electrochemical Surface Technologies, Konrad Lorenz Strasse 24, 3430 Tulln, Austria

<sup>e</sup> AIT Austrian Institute of Technology, Giefinggasse 4, 1210 Vienna, Austria

<sup>f</sup> CEST-UNLP Partner Lab for Bioelectronics, Diagonal 64 y 113, La Plata 1900, Argentina

## ARTICLE INFO

### Keywords:

PEDOT  
Graphite nanosheets  
Biosensing  
Conducting polymer  
Flexible electrode  
Metal-free

## ABSTRACT

Carbon nanomaterials are usually employed for improving the electrical and electrochemical properties of conducting polymer electrodes. However, low-cost of production, scalable simple procedures and adequate integration of the components at the molecular level within the composites become a challenge when dealing with real life applications. In this work, we present a novel strategy for producing graphite nanosheets (GNS) dispersed in the solvent employed then for the chemical synthesis of PEDOT, which allows producing composite nanofilms on plastic substrates for the construction of transparent and flexible all-polymer electrodes. By an optimized experimental procedure, we achieved a proper integration of PEDOT and GNS within ultrathin (< 100 nm) composite films and good enough conductivity to ensure adequate electrochemical response without the requirement of conducting base electrodes. We tested the performance of these platforms for real applications by developing glucose biosensors by molecular integration of supramolecular assembly of glucose oxidase and an electroactive polyelectrolyte on top of the PEDOT-GNS coatings. The incorporation of GNS does not only improve the voltammetric response of the resulting all-polymer electrodes but also produces a better integration of the electrochemically active assembly.

## 1. Introduction

Flexible electrochemical platforms have received remarkable attention over the past decade owing to their great potential in the construction of wearable and implantable devices for predictive analytics and high-performance personalized medicine [1–3]. For those purposes, flexible electronics requires a conjunction of unique properties such as light weight, high flexibility and mechanical adaptability. Thus, traditional metal electrodes and other rigid substrates can be limited in their use in some specific practical applications, like stretchable or implantable sensors [4,5]. Within this scenario, a highly attractive alternative is the use of conducting polymers (CPs) for the fabrication of “all-polymer” metal-free electrodes for bioelectronics and biosensing [6–11].

In particular, poly(3,4-ethylenedioxythiophene) (PEDOT) is a CP that has received enormous attention due to its high conductivity [12–14], good transparency [15] and stability and its excellent electroactivity in neutral media [11,16]. These properties combined with a good compatibility with biomolecules, such as enzymes, make PEDOT an appropriated polymer in the design of biosensing platforms [17]. Also, because of the remarkable conductivity of PEDOT, it is possible to construct bioelectrochemical devices without metallic substrates [18–21], which represents a great advantage in the design of low cost sensing platforms with a high degree of flexibility and transparency [16,22].

Furthermore, an improvement of the electrical, electrochemical and mechanical properties is found when conducting polymers are combined with carbon nanomaterials [23,24]. Within these materials,

\* Corresponding authors at: Instituto de Investigaciones Fisicoquímicas Teóricas y Aplicadas (INIFTA), Fac. de Cs. Exactas, Universidad Nacional de La Plata, CONICET, 64 y Diag. 113, 1900 La Plata, Argentina.

E-mail addresses: [wmarmi@inifta.unlp.edu.ar](mailto:wmarmi@inifta.unlp.edu.ar) (W.A. Marmisolle), [azzaroni@inifta.unlp.edu.ar](mailto:azzaroni@inifta.unlp.edu.ar) (O. Azzaroni).

<https://doi.org/10.1016/j.apsusc.2020.146440>

Received 7 March 2020; Received in revised form 21 April 2020; Accepted 22 April 2020

Available online 30 April 2020

0169-4332/ © 2020 Elsevier B.V. All rights reserved.

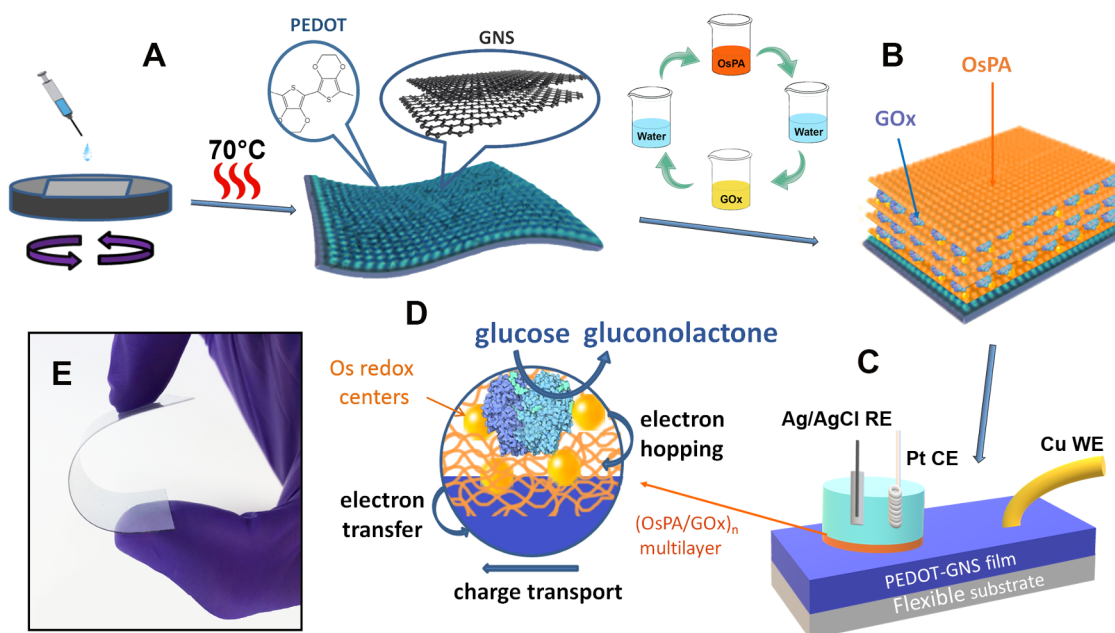


**Fig. 1.** Scheme of the steps followed for the construction of the biosensor: (A) Spin-coating deposit of the monomer-GNS mixture previous to the polymerization and (B) LbL assembly of OsPA and GOx on the PEDOT-GNS substrates. (C) Experimental setup for the voltammetric measurements in a three-electrode cell. (D) Scheme of the different charge transport mechanisms taking place in the bioelectrocatalysis of the glucose oxidation. (E) Photograph of the PEDOT-GNS platforms synthesized in this work.

carbon nanotubes (CNTs), graphene oxide (GO), and reduced graphene oxide (rGO), have been extensively employed to enhance the performance of PEDOT platforms with biosensing purposes [25–29]. Thus, the carbon-based materials usually confer good mechanical frameworks with adequate electronic properties whereas conducting polymers provide electroactivity, flexibility and capacity of acting as dispersion agents preventing the nanomaterial aggregation [23]. However, obtaining these carbon nanomaterials habitually implies complicated and expensive procedures or requires complex conditions such as high temperatures or sophisticated instruments [30–32]. Other promising material for the design of biosensors is graphite nanosheets (GNS), which refers to 2D graphite material often obtained by simple liquid-exfoliation of graphite [33–35]. Its excellent conductivity and large superficial area make GNS a suitable material for the construction of enzymatic biosensing platforms since it may enhance the immobilization of enzymes in the polymer matrix and their connectivity with the substrate.

On the other hand, a frequent issue when dealing with composite nanomaterials is the problem of achieving a proper intimate integration of both components within the films [23]. Several strategies have been presented for integrating PEDOT with carbon nanomaterials in the construction of conducting/electroactive films. In this regard, some authors have prepared composite films from mixed dispersions of PEDOT or PEDOT:PSS and carbon nanomaterials employing several strategies, such as vacuum-filtration [36], spray coating [22] and spin-coating [37], achieving different degree of integration. Even when both components are put into contact by producing mixed stable dispersions, aggressive chemical or thermal post-treatments are required for enhancing the electronic properties of the composite films by molecular reorganization [38]. On the other hand, electropolymerization of EDOT on electrodes previously modified with carbon nanomaterials [39,40] or performing the electrosynthesis in the presence of the nanomaterial [41] seem to ensure a proper integration at the molecular level. However, these methods require conducting substrates and they result difficult to scale-up.

Within this framework, herein we propose a simple method for producing graphite nanosheets (GNS) dispersions that can be directly

employed as solvent in the chemical polymerization of EDOT, yielding conducting composite films by spin-coating on plastic substrates. Mixing GNS and EDOT in butanol allows for a suitable molecular integration in thin films, which are then polymerized by soft thermal treatment. In this way, flexible, transparent and highly conducting electrochemical platforms with enhanced mechanical properties are easily prepared. The supramolecular LbL assembly of a redox polyelectrolyte and glucose oxidase was employed for evaluating the capabilities of the all-polymer PEDOT-based platforms in biosensing applications. The incorporation of GNS does not only improve the voltammetric response of the resulting all-polymer electrodes but also produces a better integration of the electrochemically active supramolecular assembly allowing the effective glucose sensing.

## 2. Experimental details

### 2.1. Reagents and materials

Fe(III) tosylate butanol solution (Clevios CB 40 V2, Heraeus Deutschland GmbH & Co. KG), n-butanol (ACS, Merck), pyridine (ACS, Biopack) and EDOT (97%, Sigma-Aldrich) were employed for the polymerization. Glucose oxidase (GOx) was purchased from Calzyme, and D-(+)-glucose was obtained from Anedra. Expanded graphite was purchased from Carbon Lorraine. Graphite (C2030519P4) and silver (C2081126P2) inks were purchased from Gwent Group (Pontypool, UK). All other reagents were of analytical grade. A 1 M glucose solution equilibrated in anomers was prepared in HEPES buffer of pH = 7.4. The complex [Os(bpy)<sub>2</sub>Cl(PyCOH)]Cl (PyCOH = Pyridine-4-aldehyde) and osmium-modified polyallylamine (OsPA) were prepared as previously reported [42]. The stoichiometry ratio between the osmium complex and the allylamine monomer was 1:60. The OsPA concentration was evaluated spectrophotometrically at  $\lambda = 495 \text{ nm}$  ( $\epsilon = 8500 \text{ M}^{-1} \text{ cm}^{-1}$ ). The pH of the polyelectrolyte solution was adjusted to 7.0 by adding NaOH.

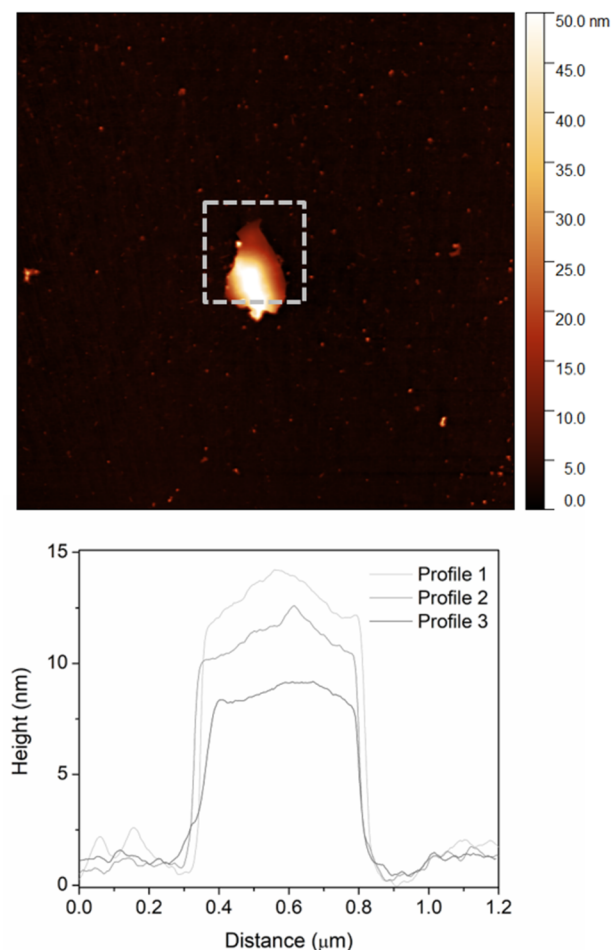


Fig. 2. Topography AFM images (10x10  $\mu\text{m}$ ) of a sample of the carbon nanomaterial resulting from the exfoliation of expanded graphite in butanol deposited on a clean Si substrate. (B) Height profiles of graphite nanosheets flake observed in the AFM image.

## 2.2. Construction of PEDOT and PEDOT-GNS conducting films

PEDOT films were prepared by *in situ* polymerization of EDOT monomer solutions deposited by spin-coating on 0.2 mm-thickness cellulose acetate sheets substrates, using a commercial spin coater (Laurell WS-400B). Before film deposition, substrates were cleaned with ethanol and Milli-Q water. A stock oxidant solution was prepared by mixing 7.5 ml of 40%  $\text{Fe}^{(\text{III})}$  tosylate butanol solution (CB 40, Clevios), 2.2 ml of butanol and 165  $\mu\text{L}$  of pyridine [10]. For the PEDOT films preparation, 915  $\mu\text{L}$  of the oxidant solution was mixed with 12.5  $\mu\text{L}$  of EDOT monomer, then homogenized in a vortex and filtered with a pore diameter of 0.2  $\mu\text{m}$  membrane. The resultant mixture was immediately deposited by spin coating employing rotation rates between 1000 and 5000 rpm for 1 min and an acceleration of 500 rpm  $\text{s}^{-1}$ . Then, the substrates were heated at 70  $^{\circ}\text{C}$  for 15 min producing a change in the color of the films from brown to green [15]. The film-coated substrates were rinsed with Milli-Q water twice and dried with  $\text{N}_2$  flow. To prepare the PEDOT-GNS films, 5 mg of expanded graphite were dispersed in 5 ml of butanol by probe ultrasonication using a VCX130 Vibra-Cell (Newtown, USA) at 120 W for 15 min. Then, different volumes of this stock dispersion were added to the polymerization mixture, reaching carbon loadings of 100 and 180  $\mu\text{g}/\text{mL}$ .

## 2.3. Resistance measurements upon bending

The electrical resistance was measured on different substrates as

they were bent. To this end, PEDOT, PEDOT-GNS, graphite and Ag films were deposited onto rectangular acetate sheets ( $5 \times 1 \text{ cm}^2$ ). These films were placed forming a semicircle of 7.5 mm radius. The extremes were connected to a multi-meter (Keithley) and the resistance was measured. Then, both sides of the films were pushed in, diminishing the radius of the semicircle. The resistance was registered for radii between 7.5 and 1 mm, respectively. The graphite and Ag films were prepared by screen-printing of graphite and silver inks onto 0.2 mm-thickness cellulose acetate sheets with an Aurel 900 screen-stencil printer (Modigliana, Italy).

## 2.4. Atomic force microscopy (AFM)

Atomic force microscopy was employed to determine the dimensions of GNS and the thicknesses of PEDOT and PEDOT-GNS films. AC mode AFM images were acquired in a dry air environment with a Keysight 9500 microscope. AC160TS (Al-coated, 300 kHz nominal frequency, 40 N/m nominal spring constant, Olympus) AFM probes were used. Samples were prepared on Si and glass substrates cleaned with basic

piranha solution. To prepare the GNS samples, a drop of a 100  $\mu\text{g}/\text{ml}$  dispersion of the carbon material in butanol was deposited on a Si substrate and the solvent was evaporated at room temperature.

## 2.5. Thermogravimetric analysis (TGA)

Thermogravimetric Analysis was performed employing a Q 500 Automatic Sample Processor (TA Instruments). The samples were heated from 22 to 790  $^{\circ}\text{C}$  under  $\text{N}_2$  flow.

## 2.6. Preparation of (OsPA/GOx)*n* multilayers electrically wired to the conducting films

Layer-by-layer (LbL) assemblies mediated by electrostatic interactions [45–48] were built up onto the PEDOT and PEDOT-GNS conducting platforms by alternate dipping in OsPA and GOx solutions. In order to confer negative charge to the PEDOT and PEDOT-GNS surfaces, the substrates were firstly incubated in 1 mg/ml poly(sodium 4-styrenesulfonate) (PSS) solution for 30 min and then rinsed with deionized water. As proved by contact angle measurements, the PSS adsorption yielded an increase of the hydrophilicity of the PEDOT and PEDOT-GNS surfaces (see Fig. S1). PSS-modified platforms were incubated in 0.3 mg/ml OsPA solution for 15 min, and rinsed with deionized water. Then, they were incubated in 1 mg/ml GOx solution in 20 mM HEPES and 0.1 M KCl at pH 7.4 for 15 min, followed by rinsing with deionized water. This procedure was repeated *n* times to obtain *n* (OsPA/GOx) bilayers. In all cases, the multilayer assemblies were finished with OsPA as the outermost layer to improve the charge transport through the redox multilayer and the bioelectrocatalytic activity [49,50], yielding (OsPA/GOx)<sub>*n*</sub>/OsPA configurations.

## 2.7. Electrochemical measurements

Cyclic voltammetry experiments were performed with an AUTOLAB potentiostat using a three-electrode array in a 2-mL capacity Teflon electrochemical cell equipped with a platinum counter electrode and a Ag/AgCl reference electrode from BASi (Indiana, USA). All electrochemical experiments were carried out at room temperature (22  $^{\circ}\text{C}$ ) in a 20 mM HEPES and 0.1 M KCl buffer solution at pH = 7.4.  $\text{N}_2$  bubbling was used to remove dissolved  $\text{O}_2$  from the glucose solutions for at least 30 min before using, and for 10 min between successive measurements.

## 3. Results and discussion

Flexible conducting platforms based on PEDOT and GNS were synthesized on acetate sheets and evaluated for biosensing applications.

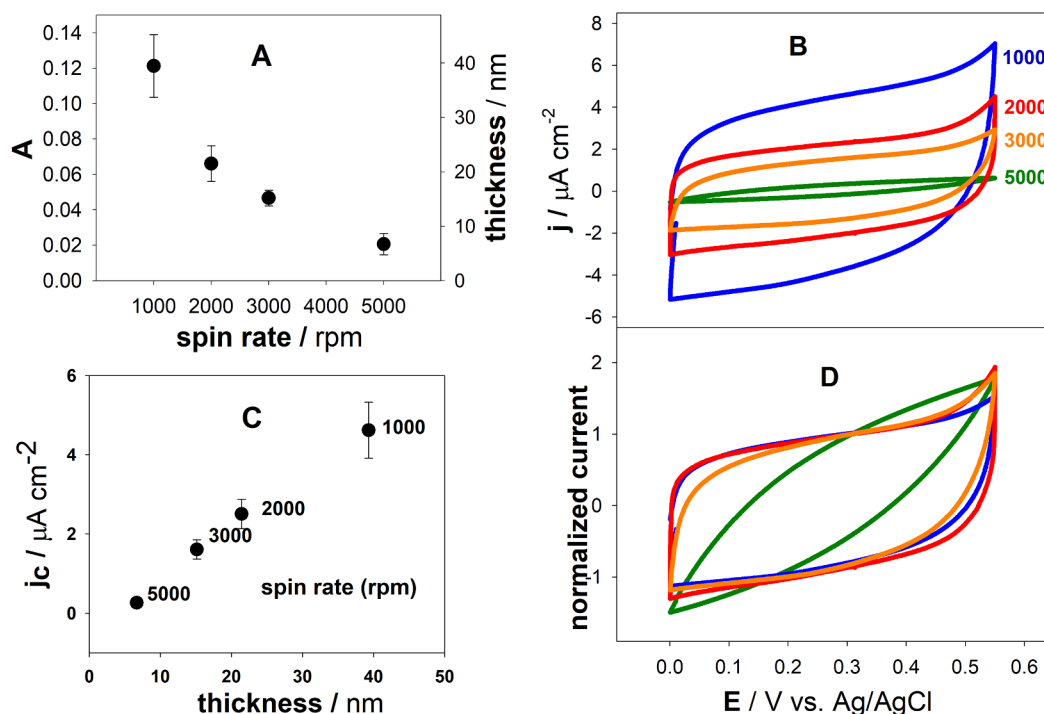


**Fig. 3.** (A) Absorbance at  $\lambda = 780$  nm and estimated thickness as a function of the spin-coating speed. (B) Cyclic voltammetry at  $5 \text{ mV s}^{-1}$  of PEDOT films deposited at spin rates between 1000 and 5000 rpm. (C) Capacitive current as a function of the thickness (the maximum thickness corresponds to the minimum spin rate). (D) Normalized voltammograms. The bars correspond to the SD of three measurements on different regions of the same substrate.

Firstly, GNS were obtained and incorporated into the PEDOT-polymer matrix during chemical synthesis on flexible acetate sheets. Then, the characteristics of the resulting composite (PEDOT-GNS) and pristine PEDOT films were studied by different techniques to evaluate the influence of the carbon nanomaterial on the stability, flexibility, and electrochemical response of the platforms. Finally, electronically wired OsPA/GOx layer-by-layer (LbL) assemblies were built on the conducting platforms to evaluate their performance as electrochemical biosensing platforms. In Fig. 1, the construction process of the PEDOT-GNS conducting platforms (A) and the (OsPA/GOx)<sub>n</sub> bioelectrocatalytic interface (B) are depicted. This figure also shows the experimental electrochemical array (C), a scheme of the transport mechanism in the bioelectrochemical coating (D) (see below) and a picture of the PEDOT-modified plastic substrate (E).

### 3.1. Platforms characterization

#### 3.1.1. Graphite nanosheets

GNS were obtained from exfoliation of expanded graphite by probe sonication in 1-butanol. As described previously by Colman and coworkers, good solvents for exfoliation are those whose Hansen solubility parameters (which are related to the dispersive, polar and hydrogen bonding contributions to the cohesive energy density of a material) match reasonably well to those for graphene and graphite [35,51]. Since the total Hansen's solubility parameter of 1-butanol is nearly equal to that of graphite, the exfoliation is facilitated [52]. The carbon material resulting from this procedure was characterized by AFM. To this end, a drop of a 100  $\mu\text{g/ml}$  dispersion of the carbon material in butanol was deposited on a Si substrate and the solvent was evaporated at room temperature. Samples consisted of dispersed material with a variety of dimensions with lateral sizes from about 25 nm to 1  $\mu\text{m}$  (Fig. 2). Graphite flakes presented heights around 10 nm ( $< 30$  graphene layers [53]), demonstrating the quality of exfoliation which is in accordance with graphite nanosheets dispersions prepared by other ultrasound procedures [54,55].

#### 3.1.2. PEDOT and PEDOT-GNS platforms

PEDOT films of different thicknesses were deposited on cellulose acetate flexible sheets by changing the spin-coating speed. Controlling the thickness of the polymer film is an important issue for the construction of biosensing platforms based on conducting polymers since it determines different properties of the electrode such as transparency, electrical resistance and electrochemical capacitance. In particular, finding a good compromise between the last two parameters may be critical in the efficiency of an electrochemical biosensor. On one hand, conducting polymer-based electrodes have a capacitive current that is proportional to the thickness of the polymer film [56]. This current superposes with the biocatalytic current and a high value of it may decrease the sensibility of the electrode [16]. On the other hand, the resistance of the polymer film increases as the thickness decreases. A high resistance of the base electrode generates a slope in the potential-current response that deforms the voltammetric profile (see Fig. 3).

To evaluate these aspects PEDOT films were deposited by spin coating employing different rotation speeds between 1000 and 5000 rpm, respectively. Then, UV/Vis spectra were measured and cyclic voltammetry was performed in buffer solution. In Fig. 3A the absorbance values of the films at 780 nm are shown for the different deposition conditions. A marked increase of the absorbance of the platforms with the decrease of the spin-coating speed is observed, indicating that thicker films are obtained at lower speeds. However, all films employed in this work show a high degree of transparency, with transmittance values between 75% and 95% in the UV/vis region. Film thickness estimated from AFM measurements (see Section S2 in Appendix A) are also included in Fig. 3A.

In Fig. 3B the voltammetric responses of the films obtained at the different spin rates are shown. In agreement with previous works on conducting films on metal substrates, it is observed that the capacitive current linearly increases with the thickness of the film (Fig. 3C). In principle, this aspect would suggest similar electrochemical connectivity for all the films. However, when analyzing the normalized voltammograms (dividing the current by the value at 0.3 V) (Fig. 3D),

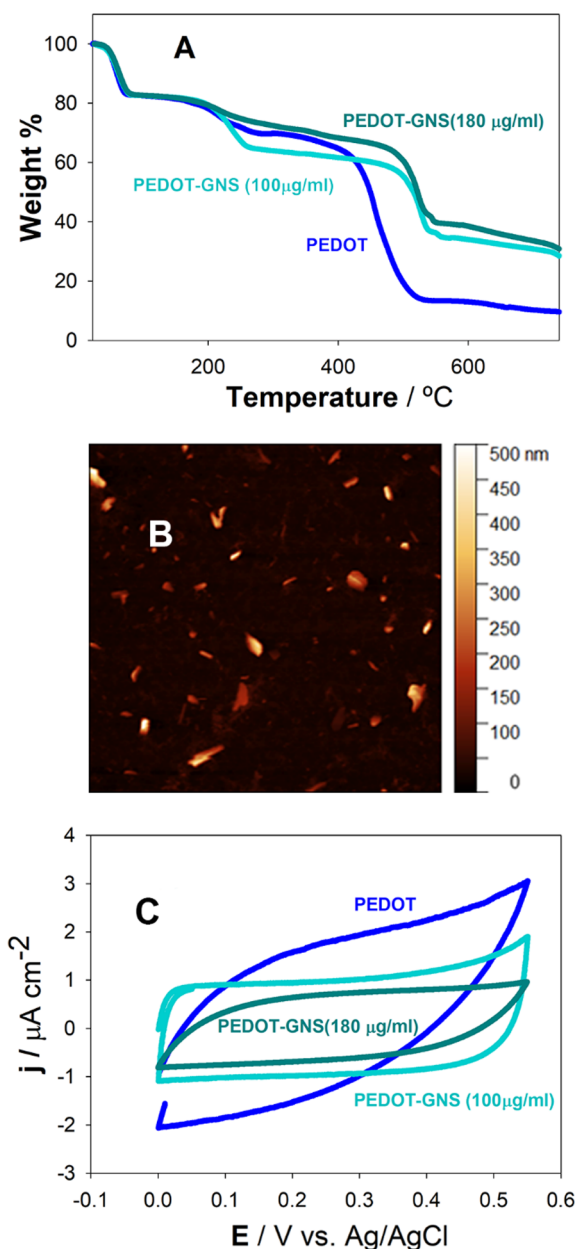


**Fig. 4.** (A) TGA curves for PEDOT and PEDOT-GNS with different amount of GNS in the polymerization mixture. The heating was done under  $\text{N}_2$  flow. (B) AFM topography image of the PEDOT-FLG film ( $12 \mu\text{m}^2$ , height range 500 nm) (C) Cyclic voltammograms at  $5 \text{ mV s}^{-1}$  of PEDOT and PEDOT-GNS films deposited on cellulose acetate sheets in 20 mM HEPES + 0.1 M KCl buffer at  $\text{pH} = 7.4$ .

clear differences appears for the different thicknesses. The voltammogram shape goes from rectangular to oval as the thickness of the film decreases, what is related to an increase of the film resistance.

These results indicate that the procedure employed here is a suitable method to generate transparent all-polymer conducting PEDOT platforms with a precise control of the film thickness. The electroactive polymer film thickness being a critical parameter for the bioelectrochemical sensing performance of the polymer-based electrodes, it needs to be optimized. In the present case, the best condition for the construction of the base electrodes was found for the films deposited at 2000 rpm (thickness  $\sim 20 \text{ nm}$ ), as a result of the compromise between a low capacitive current and a suitable voltammetric response.

Having optimized the PEDOT film thickness for the electrochemical platforms, we then studied the incorporation of the GNS into the

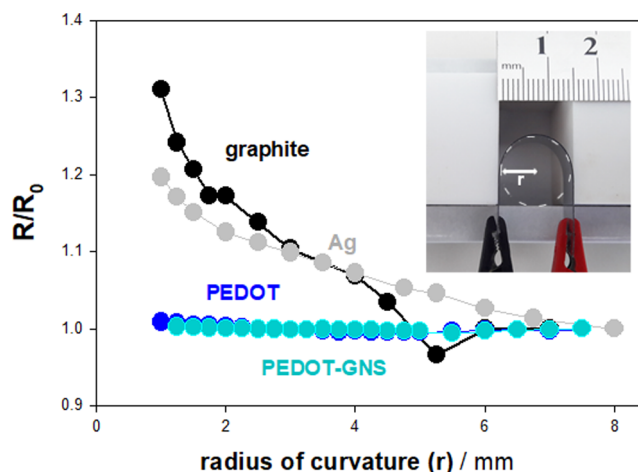


**Fig. 5.** Relative changes in the resistance of the films as a function of the radius of curvature.  $R_0$  is the value of the resistance at the initial conditions. The picture shows the condition at which the sheet is bended between two blocks defining a radius of curvature of 7.5 mm. Further bending conditions (lower radius values) were obtained by moving the blocks closer.

conducting polymer matrix with the aim of improving the electrochemical properties of the PEDOT-based platforms. Hybrid (PEDOT-GNS) films were synthesized by directly adding the GNS suspension to the monomer-oxidant solution before the spin-coating procedure. To confirm the incorporation of the GNS, TGA measurements were performed. In Fig. 4A, the curves for PEDOT and PEDOT with two different amounts of GNS (100 and 180  $\mu\text{g/ml}$  in the polymerization mixture) are shown. The three samples show mass losses below 200  $^\circ\text{C}$  which may be attributed to solvent loss. The major weight loss occurs between 380  $^\circ\text{C}$  and 540  $^\circ\text{C}$  for PEDOT and between 440  $^\circ\text{C}$  and 570  $^\circ\text{C}$  for PEDOT-GNS samples showing that the addition of GNS to the polymer increases (by about 70  $^\circ\text{C}$ ) the decomposition temperature of the material. This means that PEDOT-GNS composites have better thermal stability than pristine PEDOT. Moreover, there is a total mass loss of 90% for PEDOT film at 740  $^\circ\text{C}$  while for the PEDOT-GNS materials it is 72% for the 100 mg/ml solution and 69% for the 180 mg/ml solution, meaning an approximate GNS content of 18% and 21% w/w respectively.

PEDOT and PEDOT-GNS hybrid films topography was also characterized by AFM. In Fig. 4B the topography image of the PEDOT-GNS film is shown. Graphite nanosheets flakes with heterogeneous sizes (lateral dimensions from below 100 nm to 1.5  $\mu\text{m}$ ), are distributed over the surface. The roughness of the films was quantified from the AFM images. The presence of the GNS significantly increases the roughness of the films: PEDOT-GNS film had a roughness (RMS value) of  $(33 \pm 1) \text{ nm}$ , approximately twice the value of  $(15 \pm 1) \text{ nm}$  obtained for the PEDOT film.

After the integration of GNS into the polymer matrix was confirmed, the electrochemical performances of the films were compared. In Fig. 4C, the voltammograms of the PEDOT and PEDOT-GNS films are shown. The incorporation of GNS to the polymer matrix improves the electrochemical response of the film, showing a more rectangular-shaped voltammetric response.

Finally, the flexibility of the different materials in terms of the film electrical resistance was evaluated. For this purpose, the effect of bending on PEDOT and PEDOT-GNS platforms was studied by varying the curvature of the substrate as the film resistance was measured between two fixed spots. The same procedure was carried out with silver and graphite films deposited on the same cellulose acetate sheets that were used to construct the polymer platforms with comparative purposes. In Fig. 5, relative resistance changes of the different materials as a function of the curvature radius are presented. The results indicate excellent relative flexibility for both PEDOT and PEDOT-GNS films. Resistance values have very little changes when the films are bent even

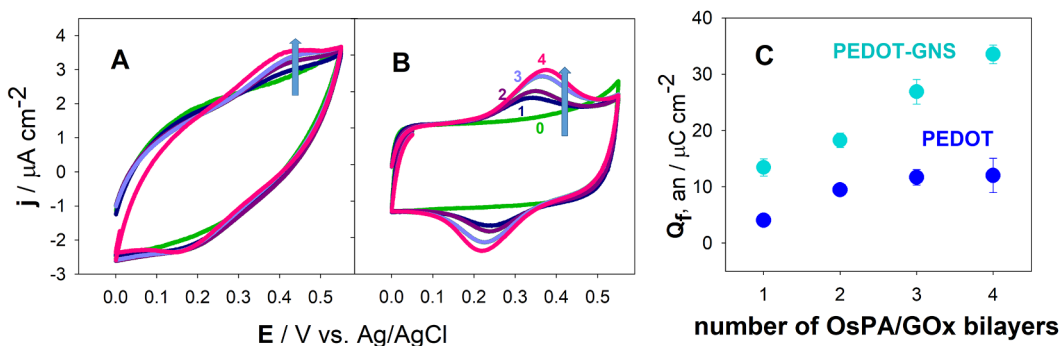


Fig. 6. Cyclic voltammetry at  $5 \text{ mV s}^{-1}$  for PEDOT (A) and PEDOT-GNS (B) modified with  $(\text{OsPA}/\text{GOx})_n/\text{OsPA}$  with different number of bilayers ( $n$ ) in  $20 \text{ mM HEPES} + 0.1 \text{ M KCl}$  buffer of  $\text{pH} = 7.4$ . (C) Anodic integrated charge ( $Q_{f, \text{an}}$ ) of the voltammograms as a function of the number of bilayers ( $n$ ) corresponding to the configuration  $\text{PEDOT}(-\text{GNS})/\text{PSS}/(\text{OsPA}/\text{GOx})_n/\text{OsPA}$ . Bars correspond to the SD of 3 different voltammograms.

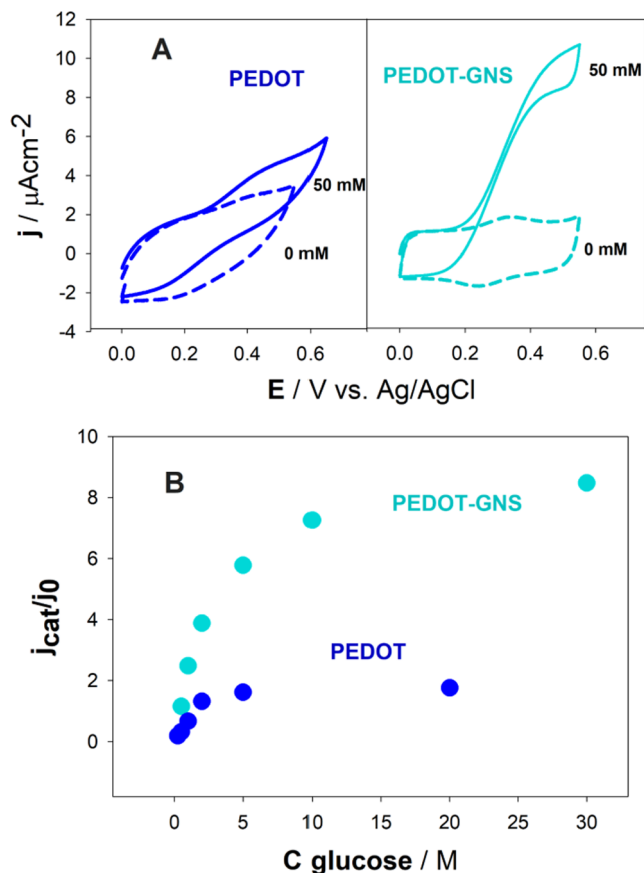


Fig. 7. (A) Bioelectrocatalytic response (density current vs. applied potential) of the  $\text{PEDOT-GNS}/\text{PSS}/(\text{OsPA}/\text{GOx})_1/\text{OsPA}$ -modified electrode in the presence of increasing concentrations of glucose. Electrolyte:  $20 \text{ mM HEPES}$  buffer ( $\text{pH} 7.4$ ) +  $0.1 \text{ M KCl}$ . (B) Catalytic current density,  $j_{\text{cat}}$ , as a function of the glucose concentration for 1, 2 and 4 bilayers. This current is defined as  $j_{\text{cat}} = j_{\text{max}} - j_0$ , where  $j_0$  is the current density in absence of glucose. Solid lines correspond to the fittings to the Michaelis-Menten model (see Appendix).

at very small radii ( $< 1\%$  for a  $1 \text{ mm}$  radius). On the contrary, Ag- and graphite-ink electrodes show mayor changes in the resistance as the electrode is bent (about  $30\%$  for Ag and  $20\%$  for graphite). No appreciable macroscopic fissures were observed on the PEDOT-GNS films after the bending tests neither a memory effect in terms of the resistance, which only increase  $1.0 \pm 0.5\%$  after a bending cycle. This last observation is in agreement with other flexible conducting platforms based on PEDOT composites that showed a resistance increment of  $1.2 \pm 0.4\%$  after bending [16].

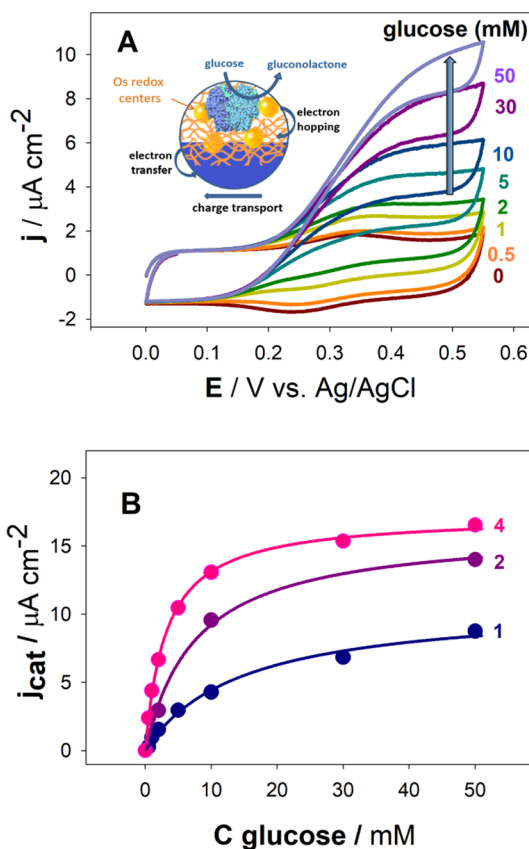


Fig. 8. (A) Bioelectrocatalytic response for PEDOT (left) and PEDOT-GNS (right) electrodes modified with one  $\text{OsPA}/\text{GOx}$  bilayer in the absence and presence  $50 \text{ mM}$  of glucose. (B)  $j_{\text{cat}}/j_0$  ratio as a function of the glucose concentration for a 4-bilayers  $\text{OsPA}/\text{GOx}$  assembly on PEDOT and PEDOT-GNS electrodes.

### 3.2. Construction of bioelectrocatalytic nanoarchitectures onto PEDOT and PEDOT-GNS platforms

The PEDOT and PEDOT-GNS films described above were employed as platforms for the assembly of bioelectrocatalytic nanoarchitectures for glucose biosensing. To this end, the layer-by-layer (LbL) assembly technique, a well-established nanoconstruction method [57–61], was used for the adsorption of GOx (a redox enzyme that catalyze the oxidation of glucose) and OsPA (a counter-polyelectrolyte that bears redox mediator groups). The LbL assembly is a versatile bottom-up technique for the non-covalent immobilization of functional biomacromolecules

into thin films, ensuring the biological activity and accessibility of the analyte to the active sites of the biomacromolecule [45,62]. This functionalization method is compatible with the production of miniaturized devices, which could be also developed on the basis of the PEDOT/GNS flexible platforms.

Redox mediators are an essential component in sensors based on redox-enzymes, which are traditionally used for the detection of glucose, lactate and cholesterol, among others. The redox mediators should fulfill several requirements: they should be stable at both oxidation states, they should assure a fast electron transfer process both to the electrode surface and to the redox-enzyme. Polypyridine osmium complexes are stable at both oxidation for long periods of time in contrast to ferrocene complexes, frequently used in these type of sensors [63], they show a reversible electrochemical behavior and they are able to re-oxidize glucose oxidase with rate constant values higher than  $10^5 \text{ M}^{-1} \text{ s}^{-1}$  [64]. In particular, the complex used in this work (i.e.,  $[\text{Os}(\text{bpy})_2\text{Cl}(\text{PyCOH})]\text{Cl}$ ) has a rate constant of  $3.7 \cdot 10^5 \text{ M}^{-1} \text{ s}^{-1}$  [42]. On the other hand, the presence of a carbonyl group allows the coupling to the polyallylamine, leading to the OsPA polycation. Its flexibility and positive charge facilitate the interaction with glucose oxidase, negatively charged at the working pH. In this way the OsPA retains the ability to re-oxidize glucose oxidase and to build multilayer systems.

Firstly, the voltammetric response in buffer solution in the absence of  $\text{O}_2$  was studied for systems with different numbers of OsPA/GOx bilayers. In Fig. 6, voltammograms taken at  $5 \text{ mV s}^{-1}$  of the modified PEDOT and PEDOT-GNS platforms are presented. Both the oxidation and reduction current peaks of the osmium bearing groups from OsPA increases with the number of OsPA/GOx bilayers, evidencing a good connectivity between the successive bilayers resulting from the electron hopping between the redox centers.

Interestingly, an improvement in the voltammetric response of the LbL assembly is observed when comparing the PEDOT and PEDOT-GNS platforms. The incorporation of GNS to the conducting film led to a better definition of the osmium oxidation and reduction waves and a decrease of the separation between the anodic and the cathodic peaks (of around 140 mV for voltammograms recorded at  $5 \text{ mV s}^{-1}$ ). In addition, there is an increase of the integrated faradaic charge of the Os oxidation peak ( $Q_{f, \text{an}}$ ) when the LbL assembly is prepared on the PEDOT-GNS composited compared with the assembly on the PEDOT platform (Fig. 6C). For 4 bilayers-assembly, the  $Q_{f, \text{an}}$  obtained for the PEDOT-GNS platform is more than 3 times higher than that one for PEDOT. Moreover, the integrated charge sequentially increases with the number of OsPA/GOx bilayers for the PEDOT-GNS modified electrode, while for the pristine PEDOT system the increment in the voltammetric charge is lower after the second bilayer. These results might be explained in terms of the increase of the roughness of the film surface when GNS are integrated into the polymer matrix leading to the incorporation of a greater amount of OsPA in the assembly. In addition, the high specific surface area of GNS (i.e.,  $800\text{--}2000 \text{ m}^2 \text{ g}^{-1}$ ) [34,65], which are also highly conducting, enhance the electrical “wiring” of the OsPA redox centers for the PEDOT-GNS platforms. Moreover, the faradaic charge obtained for three bilayers of OsPA/GOx onto the PEDOT-GNS platforms ( $20.7 \mu\text{C cm}^{-2}$ ) was similar to that reported by Flexer et al. for an OsPA/GOx system assembled under similar conditions (i.e., pH and ionic strength) but on gold electrodes ( $19.2 \mu\text{C cm}^{-2}$ ) [66].

### 3.3. Bioelectrocatalytic response

In order to evaluate the performance of the conducting polymer electrodes as biosensing platforms, the catalytic response of the PEDOT and PEDOT-GNS films modified with different numbers of OsPA/GOx bilayers was studied in the presence of  $\beta$ -D-glucose. Firstly, the LbL-modified electrodes were immersed in a buffer solution and the potential was cycled between 0.0 and 0.5 V until a stable response was observed. Then, increasing concentrations of glucose in the absence of  $\text{O}_2$  were added to the solution and the potential was cycled at  $5 \text{ mV s}^{-1}$ .

In Fig. 7A, the bioelectrocatalytic response for an electrode modified with one GOx/OsPA bilayer in the presence of different glucose concentrations for the PEDOT-GNS system is presented. The cyclic voltammograms reveal the typical waves of the glucose oxidation mediated by the electrically “wired” GOx to the electrode [45,66,67], where the whole bioelectrocatalytic process is transduced as an increment of the anodic current (more details on the electrocatalytic process are presented in the Appendix A).

In Fig. 7B the catalytic current,  $j_{\text{cat}}$  ( $j_{\text{cat}} = j_{\text{max}} - j_0$ , where  $j_{\text{max}}$  is the maximum current obtained in presence of glucose and  $j_0$  is the current density observed in the absence of glucose), as a function of the glucose concentration is showed for the same electrode modified with 1, 2 and 4 bilayers of the GOx/OsPA assembly. As can be appreciated, the bioelectrocatalytic responses displayed Michaelis–Menten behavior. The apparent Michaelis-Menten constants ( $K_m$ ) for the different architectures (Table S1) were estimated as described in the supporting information. It is observed that  $K_m$  shows its maximum value (i.e., 14 mM) for the smaller number of bilayers, which represents a wider dynamic range at expenses of a lower sensitivity for the calibration curve. On the other hand, the 4 bilayer system shows a greater sensitivity at the cost of a narrow dynamic range. The values obtained here are in the same order of magnitude (between 5 and 60 mM) than those obtained for redox mediator based on osmium complexes or ferrocene derivatives [68–70].

For both PEDOT and PEDOT-GNS platforms, a typical bioelectrocatalytic behavior is observed; i.e., the catalytic current increases with the glucose concentration until it reaches a plateau corresponding to the enzyme saturation at around 50 mM glucose. However, several differences are noted when the (OsPA/GOx) nanoarchitecture is assembled on PEDOT or PEDOT-GNS platforms. Firstly, the catalytic voltammetric response for the PEDOT-GNS system reaches more defined current plateau, whereas for the PEDOT system a distortion of this response is observed (Fig. 8A). This is a consequence of the resistance of the base electrode that deforms the voltammetric profile during the bioelectrocatalysis of glucose oxidation. A well-defined voltammetric response becomes a fundamental feature facing the bioelectroanalytical applications of the polymer platforms. Secondly, the  $j_{\text{cat}}$  obtained when the OsPA/GOx assemblies are prepared on the PEDOT-GNS electrodes is much higher than that obtained for the assemblies prepared on PEDOT platforms without GNS (Fig. S3). Moreover, PEDOT-GNS platforms showed a noticeable increase of  $j_{\text{cat}}$  as a function of the number of bilayers of the assembly, whereas the PEDOT platform showed only an increase of  $j_{\text{cat}}$  for the first two bilayers, then it remains almost constant (see Fig. S4). Lastly, in Fig. 8B, it is compared the biocatalytic current of a four bilayer OsPA/GOx assembly on PEDOT and PEDOT-GNS that shows the improvement in the bioelectrocatalytic response when the carbon nanomaterial is incorporated to the polymeric matrix. The enhancement of the bioelectrocatalytic response when GNS is added to the PEDOT platform may be a consequence of an improvement in the electrical wiring of the bioelectroactive assembly by the high surface area of conducting GNS and a higher loading of enzymes in the electrode caused by the increase of the roughness of the film.

Notable information arise from the comparison of the results obtained here with the OsPA/GOx system prepared on gold electrodes previously reported by Flexer et al. [66]. Those authors found a maximum  $j_{\text{cat}}$  of  $2.5 \mu\text{A cm}^{-2}$  at glucose saturation (50 mM) for a (OsPA/GOx)<sub>3</sub> assembly deposited on gold electrodes. On the other hand, we obtained a  $j_{\text{cat}}$  of  $14.5 \mu\text{A cm}^{-2}$  (almost six times higher) for the OsPA/GOx system prepared on the “metal-free” PEDOT-GNS platforms. This outstanding improvement of the bioelectrocatalytic response strongly evidences the important role of the GNS in the PEDOT conducting matrix for enhancing the electrical wiring of the bioelectroactive assembly. Also, in contrast to modified gold electrodes, here there is no need of mercapto-derivative compounds to work as bridge between the gold and the redox polyelectrolyte [66], improving in the long run the stability of the system.

In the last ten years a myriad of flexible glucose sensors based on the combination of highly conducting carbon materials have been presented. Some of them use metal nanoparticles to replace the enzyme/mediator system, however they have to work at alkaline pH and in most of the works the glucose selectivity (against other carbohydrates, namely mannose) is not demonstrated [71,72]; whereas other works using GOx need for the addition of a mediator in solution to obtain a response [16,73]. On the other hand, there are works that report the construction of glucose sensors with GOx electrically-wired to the electrode, but metal or graphite substrates with limited flexibility are typically used [74–76]. In the present case, not only the whole system integrated on the flexible platform is able to work at physiological conditions, but also the way in which it is constructed allows for the miniaturization of the device. Also, this concept can be extended to build enzyme logic gate-based electrochemical assays using a biocatalytic cascades to process relevant physiological parameters in the biochemical domain stimulating molecular release or the assessment of a traumatic injury [77,78].

#### 4. Conclusion

A simple method to obtain GNS dispersed in butanol and to integrate this nanomaterial into PEDOT matrices for the construction of transparent flexible all-plastic conducting platforms was presented. The addition of GNS improves the voltammetric characteristics of PEDOT platforms and allows for the adsorption of a higher amount of connected redox polymer by LbL deposition. Moreover, an enhancement of the bioelectrocatalytic response in glucose detection was observed when GNS was added to the polymer matrix suggesting a more efficient wiring of the redox centers and the enzyme, yielding better performance than similar systems prepared on gold electrodes. We believe that our approach could have profound implications in the fields of wearable and implantable sensing devices as an alternative of graphite or metal electrodes for increasing the flexibility of the devices and improving user comfort and also in the modification of fibers for developing flexible microelectrodes.

#### CRedit authorship contribution statement

**Juliana Scotto:** Conceptualization, Data curation, Writing. **Esteban Piccinini:** Conceptualization, Data curation, Writing. **Catalina Bilderling:** Methodology. **Lucy L. Coria-Oriundo:** Methodology. **Fernando Battaglini:** Investigation. **Wolfgang Knoll:** Investigation. **Waldemar A. Marmisolle:** Conceptualization, Investigation, Writing. **Omar Azzaroni:** Investigation.

#### Acknowledgements

JS and EP, acknowledge a scholarship from CONICET. CvB, FB, WAM and OA are CONICET fellows and acknowledge financial support from Universidad Nacional de La Plata (PID-X867), ANPCyT (PICT-2017-1523 and PICT2016-1680) and CEST-Competence Center for Electrochemical Surface Technologies (CEST-UNLP Partner Lab for Bioelectronics).

#### Declaration of Competing Interest

The authors declare that they have no known competing financial interests or personal relationships that could have appeared to influence the work reported in this paper.

#### Appendix A. Supplementary material

Supplementary data to this article can be found online at <https://doi.org/10.1016/j.apsusc.2020.146440>.

#### References

- [1] W.A.D.M. Jayathilaka, K. Qi, Y. Qin, A. Chinnappan, W. Serrano-García, C. Baskar, et al., Significance of nanomaterials in wearables: a review on wearable actuators and sensors, *Adv. Mater.* 31 (2019) 1–21.
- [2] Y. Yang, W. Gao, Wearable and flexible electronics for continuous molecular monitoring, *Chem. Soc. Rev.* 48 (2019) 1465–1491.
- [3] T. Someya, Z. Bao, G.G. Malliaras, The rise of plastic bioelectronics, *Nature* 540 (2016) 379–385.
- [4] E. Zeglio, A.L. Rutz, T.E. Winkler, G.G. Malliaras, A. Herland, Conjugated polymers for assessing and controlling biological functions, *Adv. Mater.* 1806712 (2019) 1806712.
- [5] J. Ha, S. Chung, M. Pei, K. Cho, H. Yang, Y. Hong, One-step interface engineering for all-inkjet-printed, all-organic components in transparent, flexible transistors and inverters: polymer binding, *ACS Appl. Mater. Interfaces* 9 (2017) 8819–8829.
- [6] Y. Hui, C. Bian, S. Xia, J. Tong, J. Wang, Synthesis and electrochemical sensing application of poly(3,4-ethylenedioxythiophene)-based materials: a review, *Anal. Chim. Acta* 1022 (2018) 1–19.
- [7] G. Kaur, R. Adhikari, P. Cass, M. Bown, P. Gunatillake, Electrically conductive polymers and composites for biomedical applications, *RSC Adv.* 5 (2015) 37553–37567.
- [8] D.A. Koutsouras, A. Hama, J. Pas, P. Gkoupidenis, B. Hivert, C. Faivre-Sarrailh, et al., PEDOT:PSS microelectrode arrays for hippocampal cell culture electro-physiological recordings, *MRS Commun.* 7 (2017) 259–265.
- [9] T. Goda, M. Toya, A. Matsumoto, Y. Miyahara, Poly(3,4-ethylenedioxythiophene) bearing phosphorylcholine groups for metal-free, antibody-free, and low-impedance biosensors specific for C-reactive protein, *ACS Appl. Mater. Interfaces* 7 (2015) 27440–27448.
- [10] J. Daprà, L.H. Lauridsen, A.T. Nielsen, N. Rozlosnik, Comparative study on aptamers as recognition elements for antibiotics in a label-free all-polymer biosensor, *Biosens. Bioelectron.* 43 (2013) 315–320.
- [11] L.D. Sappia, E. Piccinini, W. Marmisollé, N. Santilli, E. Maza, S. Moya, et al., Integration of biorecognition elements on PEDOT platforms through supramolecular interactions, *Adv. Mater. Interfaces* 4 (2017) 1700502.
- [12] J. Ouyang, Solution-processed pedot:pss films with conductivities as indium tin oxide through a treatment with mild and weak organic acids, *ACS Appl. Mater. Interfaces* 5 (2013) 13082–13088.
- [13] N. Kim, H. Kang, J.H. Lee, S. Kee, S.H. Lee, K. Lee, Highly conductive all-plastic electrodes fabricated using a novel chemically controlled transfer-printing method, *Adv. Mater.* 27 (2015) 2317–2323.
- [14] M.N. Gueye, A. Carella, N. Massonnet, E. Yvenou, S. Brenet, J. Faure-Vincent, et al., Structure and dopant engineering in PEDOT thin films: practical tools for a dramatic conductivity enhancement, *Chem. Mater.* 28 (2016) 3462–3468.
- [15] D. Choi, M. Lee, H. Kim, W. Shik Chu, D. Man Chun, S.H. Ahn, et al., Fabrication of transparent conductive tri-composite film for electrochromic application, *Appl. Surf. Sci.* 425 (2017) 1006–1013.
- [16] L.D. Sappia, E. Piccinini, C. von Binderling, W. Knoll, W. Marmisollé, O. Azzaroni, PEDOT-polyamine composite films for bioelectrochemical platforms – flexible and easy to derivatize, *Mater. Sci. Eng., C* 109 (2020) 110575.
- [17] M.J. Donahue, A. Sanchez-Sanchez, S. Inal, J. Qu, R.M. Owens, D. Mecerreyes, et al., Tailoring PEDOT properties for applications in bioelectronics, *Mater. Sci. Eng. R Rep.* 140 (2020) 100546.
- [18] N.Y. Shim, D.A. Bernards, D.J. Macaya, J.A. DeFranco, M. Nikolou, R.M. Owens, et al., All-plastic electrochemical transistor for glucose sensing using a ferrocene mediator, *Sensors* 9 (2009) 9896–9902.
- [19] I. Gualandi, M. Marzocchi, E. Scavetta, M. Calienni, A. Bonfiglio, B. Fraboni, A simple all-PEDOT:PSS electrochemical transistor for ascorbic acid sensing, *J. Mater. Chem. B* 3 (2015) 6753–6762.
- [20] W. Meng, R. Ge, Z. Li, J. Tong, T. Liu, Q. Zhao, et al., Conductivity enhancement of PEDOT:PSS films via phosphoric acid treatment for flexible all-plastic solar cells, *ACS Appl. Mater. Interfaces* 7 (2015) 14089–14094.
- [21] G. Pérez-Mitta, W.A. Marmisollé, C. Trautmann, M.E. Toimil-Molares, O. Azzaroni, An all-plastic field-effect nanofluidic diode gated by a conducting polymer layer, *Adv. Mater.* 1700972 (2017) 1–6.
- [22] T. Wang, L.-C. Jing, Q. Zhu, A. Sagadevan Ethiraj, Y. Tian, H. Zhao, et al., Fabrication of architectural structured polydopamine-functionalized reduced graphene oxide/carbon nanotube/PEDOT:PSS nanocomposites as flexible transparent electrodes for OLEDs, *Appl. Surf. Sci.* 500 (2020) 143997.
- [23] W.A. Marmisollé, O. Azzaroni, Recent developments in the layer-by-layer assembly of polyaniline and carbon nanomaterials for energy storage and sensing applications. From synthetic aspects to structural and functional characterization, *Nanoscale* 8 (2016) 9890–9918.
- [24] B.V.R.S. Subramanyam, P.C. Mahakul, K. Sa, J. Raiguru, I. Alam, S. Das, et al., Improved stability and performance of organic photovoltaic cells by application of carbon nanostructures and PEDOT:PSS composites as additional transparent electrodes, *Sol. Energy* 186 (2019) 146–155.
- [25] M. Braik, M.M. Barsan, C. Dridi, M. Ben Ali, C.M.a. Brett, Highly sensitive amperometric enzyme biosensor for detection of superoxide based on conducting polymer/CNT modified electrodes and superoxide dismutase, *Sensors Actuators, B Chem.* 236 (2016) 574–582.
- [26] S. Kumar, S. Kumar, S. Srivastava, B.K. Yadav, S.H. Lee, J.G. Sharma, et al., Reduced graphene oxide modified smart conducting paper for cancer biosensor, *Biosens. Bioelectron.* 73 (2015) 114–122.
- [27] G. Xu, Z.a. Jarjes, V. Desprez, P.a. Kilmartin, J. Travas-Sejdic, Sensitive, selective, disposable electrochemical dopamine sensor based on PEDOT-modified laser

- scribed graphene, *Biosens. Bioelectron.* 107 (2018) 184–191.
- [28] M.M. Barsan, V. Pifferi, L. Falciola, C.M.A. Brett, New CNT/poly(brilliant green) and CNT/poly(3,4-ethylenedioxythiophene) based electrochemical enzyme biosensors, *Anal. Chim. Acta* 927 (2016) 35–45.
- [29] A. Wong, A.M. Santos, T.A. Silva, O. Fatibello-Filho, Simultaneous determination of isoproterenol, acetaminophen, folic acid, propranolol and caffeine using a sensor platform based on carbon black, graphene oxide, copper nanoparticles and PEDOT:PSS, *Talanta* 183 (2018) 329–338.
- [30] A.M.K. Esawi, M.M. Farag, Carbon nanotube reinforced composites: potential and current challenges, *Mater. Des.* 28 (2007) 2394–2401.
- [31] X. Su, G. Wang, W. Li, J. Bai, H. Wang, A simple method for preparing graphene nano-sheets at low temperature, *Adv. Powder Technol.* 24 (2013) 317–323.
- [32] D. Long, W. Li, L. Ling, J. Miyawaki, I. Mochida, S. Yoon, Preparation of nitrogen-doped graphene sheets by a combined chemical and hydrothermal reduction of graphene oxide, *Langmuir* 26 (2010) 16096–16102.
- [33] A. Bianco, H.M. Cheng, T. Enoki, Y. Gogotsi, R.H. Hurt, N. Koratkar, et al., All in the graphene family – a recommended nomenclature for two-dimensional carbon materials, *Carbon N. Y.* 65 (2013) 1–6.
- [34] L. Niu, J.N. Coleman, H. Zhang, H. Shin, M. Chhowalla, Z. Zheng, Production of two-dimensional nanomaterials via liquid-based direct exfoliation, *Small* 12 (2016) 272–293.
- [35] Y. Hernandez, V. Nicolosi, M. Lotya, F.M. Blighe, Z. Sun, S. De, et al., High-yield production of graphene by liquid-phase exfoliation of graphite, *Nat. Nanotechnol.* 3 (2008) 563–568.
- [36] W. Fan, L. Liang, B. Zhang, C.Y. Guo, G. Chen, PEDOT thermoelectric composites with excellent power factors prepared by 3-phase interfacial electropolymerization and carbon nanotube chemical doping, *J. Mater. Chem. A* 7 (2019) 13687–13694.
- [37] X. Jiang, Z. Wang, W. Han, Q. Liu, S. Lu, Y. Wen, et al., High performance silicon-organic hybrid solar cells via improving conductivity of PEDOT:PSS with reduced graphene oxide, *Appl. Surf. Sci.* 407 (2017) 398–404.
- [38] D.J. Yun, H. Ra, J.M. Kim, J.H. Lee, S.H. Park, J. Hwang, et al., A study on distinctive transition mechanism of sulfuric acid treatment on performance enhancement of poly(3,4-ethylenedioxythiophene): polystyrene based electrodes depending on multiwall carbon nanotube dose, *Appl. Surf. Sci.* 487 (2019) 480–487.
- [39] K. Krukiewicz, J.S. Bulmer, D. Janas, K.K.K. Koziol, J.K. Zak, Poly(3,4-ethylenedioxythiophene) growth on the surface of horizontally aligned MWCNT electrode, *Appl. Surf. Sci.* 335 (2015) 130–136.
- [40] G. Paterakis, D. Raptis, A. Ploumistos, M. Belekoukia, L. Sygellou, M.S. Ramasamy, et al., N-doped graphene/PEDOT composite films as counter electrodes in DSSCs: unveiling the mechanism of electrocatalytic activity enhancement, *Appl. Surf. Sci.* 423 (2017) 443–450.
- [41] J. Ma, S. Yuan, S. Yang, H. Lu, Y. Li, Poly(3,4-ethylenedioxythiophene)/reduced graphene oxide composites as counter electrodes for high efficiency dye-sensitized solar cells, *Appl. Surf. Sci.* 440 (2018) 8–15.
- [42] C. Danilowicz, E. Cortón, F. Battaglini, Osmium complexes bearing functional groups: building blocks for integrated chemical systems, *J. Electroanal. Chem.* 445 (1998) 89–94.
- [43] J. Hodak, R. Etchenique, E.J. Calvo, K. Singhal, P.N. Bartlett, Layer-by-layer self-assembly of glucose oxidase with a poly(allylamine)ferrocene redox mediator, *Langmuir* 13 (1997) 2708–2716.
- [44] E. Piccinini, C. Bliem, C. Reiner-Rozman, F. Battaglini, O. Azzaroni, W. Knoll, Enzyme-polyelectrolyte multilayer assemblies on reduced graphene oxide field-effect transistors for biosensing applications, *Biosens. Bioelectron.* 92 (2017) 661–667.
- [45] T. Berninger, C. Bliem, E. Piccinini, O. Azzaroni, W. Knoll, Cascading reaction of arginase and urease on a graphene-based FET for ultrasensitive, real-time detection of arginine, *Biosens. Bioelectron.* 115 (2018) 104–110.
- [46] E. Piccinini, S. Alberti, G.S. Longo, T. Berninger, J. Breu, J. Dostalek, et al., Pushing the boundaries of interfacial sensitivity in graphene FET sensors: polyelectrolyte multilayers strongly increase the Debye screening length, *J. Phys. Chem. C* 122 (2018) 10181–10188.
- [47] M. Tagliuzuchi, E.J. Calvo, Charge transport in redox polyelectrolyte multilayer films: the dramatic effects of outmost layer and solution ionic strength, *ChemPhysChem* 11 (2010) 2957–2968.
- [48] E.J. Calvo, V. Flexer, M. Tagliuzuchi, P. Scodeller, Effects of the nature and charge of the topmost layer in layer by layer self assembled amperometric enzyme electrodes, *PCCP* 12 (2010) 10033–10039.
- [49] A. O'Neill, U. Khan, P.N. Nirmalraj, J. Boland, J.N. Coleman, Graphene dispersion and exfoliation in low boiling point solvents, *J. Phys. Chem. C* 115 (2011) 5422–5428.
- [50] M.W. Akhtar, C.W. Park, Y.S. Kim, J.S. Kim, Facile large scale production of few-layer graphene sheets by shear exfoliation in volatile solvent, *J. Nanosci. Nanotechnol.* 15 (2015) 9624–9629.
- [51] A.H. Castro Neto, F. Guinea, N.M.R. Peres, K.S. Novoselov, A.K. Geim, The electronic properties of graphene, *Rev. Mod. Phys.* 81 (2009) 109–162.
- [52] Z.S. Wu, W. Ren, L. Gao, B. Liu, C. Jiang, H.M. Cheng, Synthesis of high-quality graphene with a pre-determined number of layers, *Carbon N. Y.* 47 (2009) 493–499.
- [53] K. Muthoosamy, S. Manickam, State of the art and recent advances in the ultrasonic-assisted synthesis, exfoliation and functionalization of graphene derivatives, *Ultrason. Sonochem.* 39 (2017) 478–493.
- [54] J. Scotto, W.A. Marmisollé, D. Posadas, About the capacitive currents in conducting polymers: the case of polyaniline, *J. Solid State Electrochem.* 23 (2019) 1947–1965.
- [55] K. Ariga, Q. Ji, T. Mori, M. Naito, Y. Yamauchi, H. Abe, et al., Enzyme nanoarchitectonics: organization and device application, *Chem. Soc. Rev.* 42 (2013) 6322–6345.
- [56] G. Decher, J.B. Schlenoff, *Multilayer Thin Films: Sequential Assembly of Nanocomposite Materials*, second ed., VCH-Wiley, Weinheim, 2012.
- [57] G. Rydzek, Q. Ji, M. Li, P. Schaaf, J.P. Hill, F. Boulmedais, et al., Electrochemical nanoarchitectonics and layer-by-layer assembly: from basics to future, *Nano Today* 10 (2015) 138–167.
- [58] K. Ariga, Y. Yamauchi, G. Rydzek, Q. Ji, Y. Yonamine, K.C.-W. Wu, et al., Layer-by-layer nanoarchitectonics: invention, innovation, and evolution, *Chem. Lett.* 43 (2014) 36–68.
- [59] E. Piccinini, J.S. Tuninetti, J. Irigoyen Otamendi, S.E. Moya, M. Ceolín, F. Battaglini, et al., Surfactants as mesogenic agents in layer-by-layer assembled polyelectrolyte/surfactant multilayers: nanoarchitected “soft” thin films displaying a tailored mesostructure, *PCCP* 20 (2018) 9298–9308.
- [60] R.M. Iost, F.N. Crespiello, Layer-by-layer self-assembly and electrochemistry: applications in biosensing and bioelectronics, *Biosens. Bioelectron.* 31 (2012) 1–10.
- [61] S.A. Merchant, D.T. Glatzhofer, D.W. Schmidtke, Effects of electrolyte and pH on the behavior of cross-linked films of ferrocene-modified poly(ethylenimine), *Langmuir* 23 (2007) 11295–11302.
- [62] Y. Nakabayashi, A. Omayu, S. Yagi, K. Nakamura, J. Motonaka, Evaluation of osmium(II) complexes as electron transfer mediators accessible for amperometric glucose sensors, *Anal. Sci.* 17 (2001) 945–950.
- [63] B. Das, K. Eswar, Prasad, U. Ramamurty, C.N.R. Rao, Nano-indentation studies on polymer matrix composites reinforced by few-layer graphene, *Nanotechnology* 20 (2009).
- [64] V. Flexer, E.S. Forzani, E.J. Calvo, S.J. Ludueña, L.I. Pietrasanta, Structure and thickness dependence of “molecular wiring” in nanostructured enzyme multilayers, *Anal. Chem.* 78 (2006) 399–407.
- [65] N. Anicet, J. Moiroux, J.-M. Savéant, Electron transfer in organized assemblies of biomolecules, *Construct. Dyn. Avidin/Biotin Co-immobil. Glucose Oxidase/Ferrocene Monolayer Carbon Elect.* 4 (1998) 7115–7116.
- [66] M. Marquitan, A. Ruff, M. Bramini, S. Herlitze, M.D. Mark, W. Schuhmann, Polymer/enzyme-modified HF-etched carbon nanoelectrodes for single-cell analysis, *Bioelectrochemistry* 133 (2020) 107487.
- [67] P.N. Bartlett, C.S. Toh, E.J. Calvo, V. Flexer, *Modelling biosensor responses*, in: P.N. Bartlett (Ed.), *Bioelectrochemistry*, John Wiley & Sons, Ltd, Chichester, UK, 2008, pp. 267–325, <https://doi.org/10.1002/9780470753842.ch8>.
- [68] G.R. VandeZande, J.M. Olvany, J.L. Rutherford, M. Rasmussen, *Enzyme Stabilization and Immobilization*, Springer, New York, New York, NY, 2017.
- [69] Q. Zhang, M. Li, Z. Wang, C. Qin, M. Zhang, Y. Li, Porous Cu<sub>2</sub>O/Ag<sub>2</sub>O (x = 1, 2) nanowires anodized on nanoporous Cu-Ag bimetal network as a self-supported flexible electrode for glucose sensing, *Appl. Surf. Sci.* 515 (2020) 1–9.
- [70] S.D. Rani, R. Ramachandran, S. Sheet, M.A. Aziz, Y.S. Lee, A.G. Al-Sehemi, et al., NiMoO<sub>4</sub> nanoparticles decorated carbon nanofiber membranes for the flexible and high performance glucose sensors, *Sensors Actuators, B Chem.* 312 (2020) 127886.
- [71] Y. Aleeva, G. Maira, M. Scopelliti, V. Vinciguerra, G. Scandurra, G. Cannata, et al., Amperometric biosensor and front-end electronics for remote glucose monitoring by crosslinked PEDOT-glucose oxidase, *IEEE Sens. J.* 18 (2018) 4869–4878.
- [72] C. Chen, Q. Xie, D. Yang, H. Xiao, Y. Fu, Y. Tan, et al., Recent advances in electrochemical glucose biosensors: a review, *RSC Adv.* 3 (2013) 4473.
- [73] J.-Y. Wang, L.-C. Chen, K.-C. Ho, Synthesis of redox polymer nanobeads and nanocomposites for glucose biosensors, *ACS Appl. Mater. Interfaces* 5 (2013) 7852–7861.
- [74] W. Gao, S. Emaminejad, H.Y.Y. Nyein, S. Challa, K. Chen, A. Peck, et al., Fully integrated wearable sensor arrays for multiplexed in situ perspiration analysis, *Nature* 529 (2016) 509–514.
- [75] N. Zhou, J.R. Windmiller, G. Valdés-Ramírez, M. Zhou, J. Haláček, E. Katz, et al., Enzyme-based NAND gate for rapid electrochemical screening of traumatic brain injury in serum, *Anal. Chim. Acta* 703 (2011) 94–100.
- [76] E. Katz, Enzyme-based logic gates and networks with output signals analyzed by various methods, *ChemPhysChem* 18 (2017) 1688–1713.